Vibro-acoustic measurements and techniques for electric automotive applications

Mathieu SARRAZIN[1]; Steven GILLIJNS[1]; Karl JANSSENS[1]; Herman VAN DER AUWERAER[1]; Kevin VERHAEGHE[2]

[1] SIEMENS INDUSTRY SOFTWARE NV, Interleuvenlaan 68, B-3001 Leuven, Belgium

[2] Inverto NV, Jacques Parijslaan 8, B-9940 Evergem, Belgium

ABSTRACT

In this study, noise and vibration measurements were carried out on a multi-phase 12/8 switched reluctance (SR) motor and analyzed with vibro-acoustic techniques. When evaluating the behavior of electric powertrains for automotive applications, it is necessary to perform a vibro-acoustic analysis, particularly in view of the acoustic comfort perceived by the driver and passengers. High frequency tonal noise can be very annoying and even causes long term damage. Therefore, the noise and vibrations must be deliberately optimized. In case of a SR motor, the radial magnetic forces between the stator and rotor are the main excitation source, yielding large deformations of the stator housing and emissions of noise. Measurements and simulation results are compared for different load conditions. The dominant vibration modes are analyzed with modal analysis techniques. The unpleasant tonal noise of the motor is objectively quantified by noise metrics. Finally, the relationship between the current profiles, radial magnetic forces, and mechanical and acoustical vibrations is investigated in order to obtain a better understanding of the mechanisms underlying the vibro-acoustic behavior of the motor.

Keywords: NVH, Electric Powertrains and Vehicles, Data Acquisition I-INCE Classification of Subjects Number(s): 11.5, 13.2, 21.7, 74.

1. INTRODUCTION

Nowadays, Switched Reluctance (SR) motors reflect a very attractive alternative to other electric motor types for automotive traction. An advantage of the SR motor is its simple design, which yields a cost-effective construction. The SR motor suffers, however, from a Noise, Vibration and Harshness (NVH) issue which has caused some concern in the automotive industry. The noise and vibration radiation produced by SR motors is one of the most crucial problems to be solved before it will find its growth into the automotive industry. The NVH properties of a SR motor depend on several factors such as machine dimensions, material properties and electromagnetic design. A NVH analysis provides an essential value towards the challenges of designing SR motors in terms of ride comfort and acoustic comfort inside a vehicle.

This paper presents the results of a detailed experimental NVH assessment of a SR motor with the aim to establish an understanding of the main noise generation and propagation mechanisms. Firstly, an acoustic noise generation process for a SR motor is presented. Next, the measurement test setup and the objectives of this research are discussed, followed by the vibro-acoustic measurement results. More in detail, a signature time and frequency analysis, a modal analysis, sound metrics and the operational deflection shapes are described for this specific type of electric driveline. Finally, some conclusions are drawn.

2. ACOUSTIC NOISE GENERATION PROCESS

A multi-phase SR motor is a type of synchronous machine, but with particular features: the field

[1] mathieu.sarrazin@siemens.com
[2] kevin.verhaeghe@inverto.com

coil is wound around the stator poles, but no coil or magnetic material is presented on the rotor. The motor works by energizing opposite stator poles, thereby generating a magnetic field. This magnetic field forces the rotor poles to rotate to the position of minimum reluctance, aligning them to the closest stator poles. By energizing consecutive stator poles, continuous rotation is generated (1). Figure 1 shows the principle for a 12/8 SR motor, which has 12 stator poles and 8 rotor poles. Considering one phase, it can be observed that two main equilibrium positions of the rotor exist. The rotor position illustrated in Figure 1a is called the unaligned position in relation to phase AA'. The position with the smallest magnetic reluctance is called the aligned position (Figure 1b). Typically, the number of rotor poles is lower than the number of stator poles, which prevents the poles from all aligning at the same time, such that, by switching the poles in an appropriate way a continuous rotary motion can be established.

(a) Unaligned position (b) Aligned position

Figure 1 - Cross-sections of the analysed 12/8 SR motor and distribution of one coil group

In a 12/8 SR motor, each of the stator phases is activated eight times per revolution. Table 1 compares other configurations, where N_p is the number of poles excited at the same time, N_e the number of electrical phases, N_t, the total number of phase excitations per revolution and O the number of times that a phase is excited per revolution:

Table 1 - Different SR motor configurations

Parameters	**Configuration**		
	8/6	**12/8**	**16/12**
$\mathbf{N_p}$	2	4	4
$\mathbf{N_e}$	4	3	4
$\mathbf{N_t}$	24	24	48
O	6	8	12

As shown in Figure 2a, the acoustic noise generation process of a SR motor consists of three steps. Generally, the torque originating from the radial magnetic forces, which are determined by the phase currents, controlled by the switching pattern, plays a dominant role in the noise generation of a SR motor. In the first step, the phase currents flowing through the stator coils generate time-varying radial forces (Equation 1) in the air gap between the stator and the rotor poles. The considered radial force F_r is proportional to the square of the phase current i:

$$F_r(\theta, l_g, i) = -\frac{1}{2} i^2 \frac{L(\theta, i)}{l_g} \quad (1)$$

where $L(\theta, i)$ is the self-inductance of a single phase in function of the rotor position θ and l_g is the air gap length between rotor and stator. In the second step, these radial forces excite vibrations in the stator which are propagated through the mechanical structure. The largest vibration levels arise when the natural modes of the stator are excited by the pulsating radial magnetic forces (Figure 2b). In the final step, the deformations of the stator and the attached components cause air vibrations resulting in pressure differences detectable by the human ear.

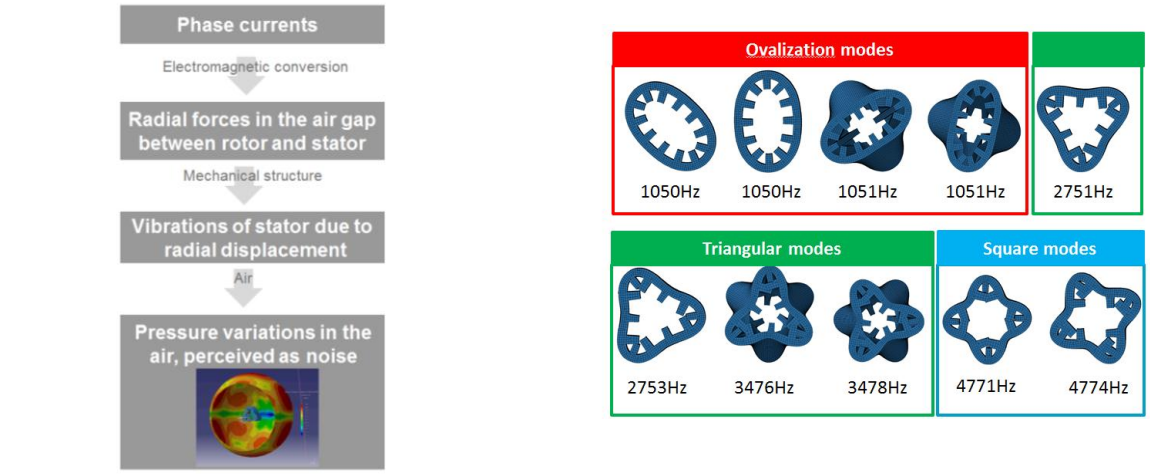

(a) Noise generation process of a SR motor

(b) Simulated finite element model of the stator mode shapes (2)

Figure 2 - Noise generation process of a SR motor with its corresponding mode shapes

Each type of SR motor has its own unique acoustic and vibration signature which is defined by several factors such as the mechanical design, the electromagnetic design and the excitation pattern of the phase currents. It is expected that a 12/8 SR motor has better NVH properties than the 8/6 configuration. In general, the natural frequencies of the square mode are higher and the 'ovalization' mode is not expected because four poles are excited at the same time resulting in a symmetric distribution. As a result, a lower noise contribution for a 12/8 configuration should be achieved in the most sensitive frequency area of the human ear.

3. EXPERIMENTAL TEST SETUP AND THE OBJECTIVES

Before presenting the vibro-acoustic analysis, this section introduces the reader to the setup and the objectives of the measurements. The setup includes two different machines, a 12/8 SR motor and 110 kW squirrel cage induction motor. It concerns a 2-pole induction motor with a modular three-level IGBT converter. A PC-based controller, a programmable powerful target PC, is used to compile graphical block diagram algorithms and run real-time. To satisfy the high performance over the full speed range, a field-oriented control (FOC) is implemented to control the induction motor. The SR drive used a conventional control technique, hysteresis current control and is coupled to the induction motor with belts. Figure 3 shows the principal parts of the test rig setup. The properties of the SR motor are described in Table 2.

Table 2 - Properties of the SR motor

Parameters	Value	Unit
E-motor dimensions (LxD)	215x256	mm
E-motor weight	50	kg
E-motor inertia	21087	$kgmm^2$
Nominal continuous power	45	kW
Maximum speed	15000	min^{-1}

In total, sixty tri-axial accelerometers were mounted on the jacket and the side panels. Furthermore, four microphones were placed: two in the near-field, two in far-field. An acoustic insulation box was placed around the SR driveline to separate the acoustic motor noise from environmental noise. To measure very accurately the rotational speed, an incremental encoder is used. Its output is measured in 2048 pulses per revolution which gives a very detailed rotational speed profile.

The main objective of the measurement campaign is to evaluate a 12/8 SR motor in terms of NVH

performance. More specific objectives are i) to verify with the help of operational deflection shapes that the square mode is the first excited mode, ii) to identify the dominant orders in different conditions, iii) to assess the tonality, loudness and sharpness with sound metrics.

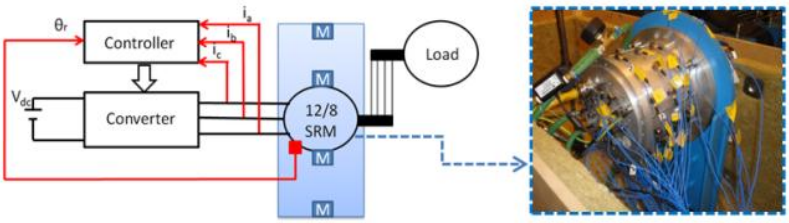

Figure 3 - Test rig with a SR drive system coupled to a two-pole induction motor

An electric motor for vehicle applications should be able to operate in the four quadrants of the speed-torque plane. In this study, motor quadrant I and II (Figure 4) are considered as they are the most used ones in automotive applications. Quadrant 1 indicates forward motoring since the torque is in the direction of motion. Quadrant 2 indicates forward braking since the torque is opposite to the direction of motion.

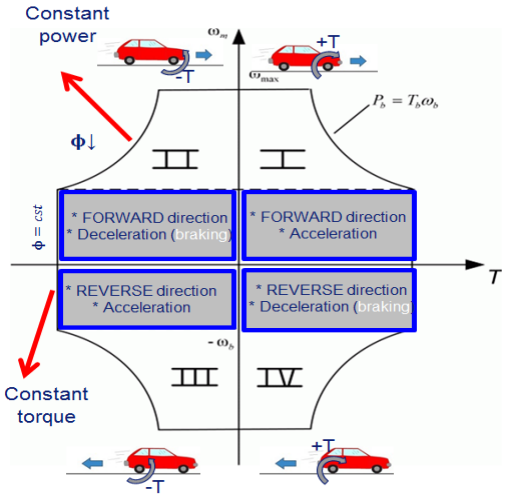

Figure 4 - Four quadrant motion control of an electric motor

In both quadrants, different torque levels from 0% to 49% were studied (Figure 5) for this type of machine.

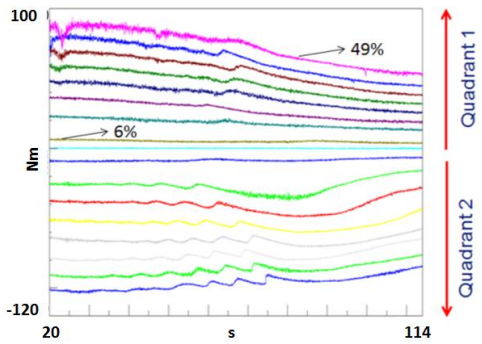

Figure 5 - Torque conditions during acceleration and deceleration in forward direction

4. VIBRO-ACOUSTIC STUDY BASED ON EXPERIMENTAL DATA

In this paragraph, both the results of a modal analysis and operational measurements in a speed range from 0 up to 10000 RPM are studied in different load conditions.

4.1 Signature time and frequency analysis

A waterfall 3D-graph is used to perform a signature frequency analysis on this particular E-motor. It is a way to present and to compare electrical data, vibration data and acoustic noise of rotating machines, like electrical powertrains. More in detail, the color map of the frequency spectra shows a dB-level as function of time or rotational speed. Figure 6a shows a waterfall spectrum of a phase current acquired during a run-up measurement. The corresponding time traces of the current waves are presented in Figure 6b.

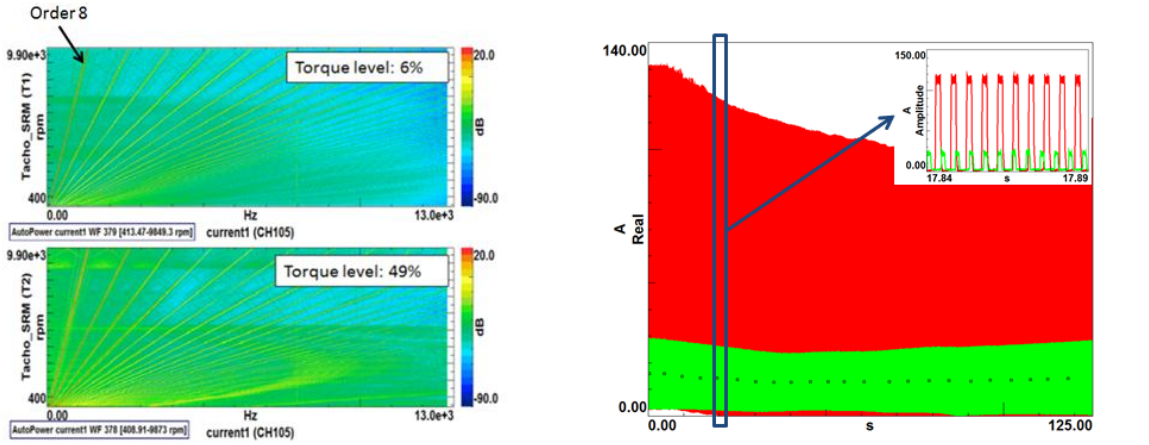

(a) Phase current spectra during run-up operations

(b) Measured phase current time profile in different load conditions: 6% (green) and 49% (red).

Figure 6 – Measured current profile with its frequency spectra in different load and speed conditions

With this kind of evaluation different characteristics can be examined. The oblique lines in Figure 6a are motor harmonics, also called orders, which are rotational speed dependent. For the points on these lines, the relation between the frequency and the rotational speed is given by

$$f = \frac{h.N.RPM}{60} \tag{2}$$

where f is the frequency in Hz, N the number of rotor poles and RPM the rotational speed in revolutions per minute (3). The number of the order h determines the slope of the line. As can be seen in Figure 6a, the 8th order is the most dominant order for a 12/8 SR motor. This is due to the fact that each of the stator phases is activated eight times per revolution in this type of SR motor.

A next step is to go more in detail with an order analysis (Figure 7) by extracting the orders from the map.

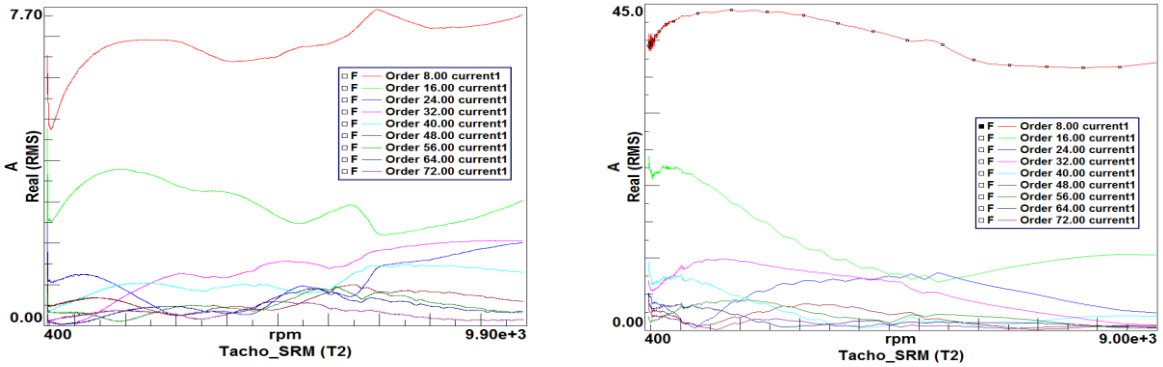

(a) Order sections for a torque level of 6%

(b) Order sections for a torque level of 49%

Figure 7 - Overview order section in different load conditions

An order section allows inspecting the behavior of single tonal components referring to the rotational speed of the motor itself. In this case the dominant order sections are calculated for a torque

level of 6% and 49%. As shown, the higher the harmonic number is, the lower the amplitude for a specific order line is.

Figure 8a shows a spectrogram of an accelerometer on the stator housing. Three phenomena can be recognized: i) 8th order harmonics, ii) resonances and iii) a kind of inverted C-shape. Figure 8b shows the corresponding acoustic noise signature in the near-field. In the proposed accelerometer signal, the resonance close to 6.3 kHz doesn't lead to increase of the acoustic power near this frequency. In fact, resonances of the stator amplify the excitation forces. The dominant resonance in this application is approximately 6.3 kHz with a corresponding square mode shape (4). This is due to the fact that four stator poles are symmetrically loaded in a 12/8 SR motor. Another resonance at 1330 Hz, an "ovalization" of the stator should not be excited in a 12/8 SR motor due to symmetry, but it is present probably due to manufacturing tolerances and rotor eccentricity [4].

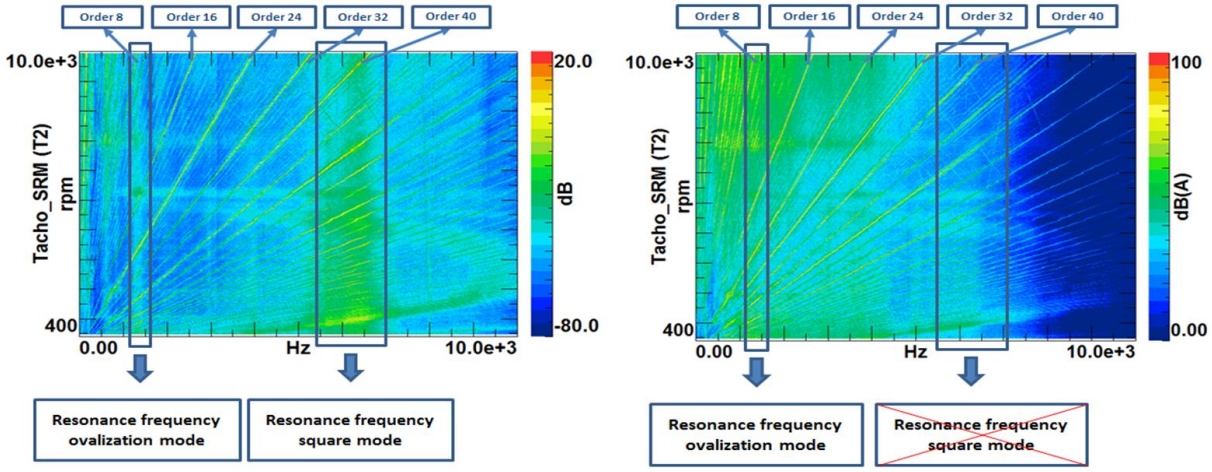

(a) PSD of an accelerometer on jacket (b) PSD of a microphone in near-field

Figure 8 – Frequency spectrum analysis in function of the rotational SR motor speed and amplitude

Another phenomenon that can be observed in Figure 8 is a feature in the form of an inverted C-shape. By analyzing it more detailed, this C-shape is mainly related to the phase current commutation process. Principally, at low and intermediate rotational speed a higher content of the current ripple is present (Figure 9). By reason of a low back electromotive force (EMF), a quite rectangular current pulse with a ripple is present and goes finally through the excited phase coils. At higher speeds, the back EMF increases. Consequently, the current pulse is no longer rectangular but becomes slightly triangular and has a much lower ripple contribution. At the end, it is also reflected in the torque profile which causes noise and vibrations. Equation 3 shows the relation that the electromagnetic torque for one phase of a SR motor is proportional to the current

$$T = \frac{i^2 dL}{2d\theta} \tag{3}$$

considering i = the electrical current, L = the motor inductance and θ = the rotor angle.

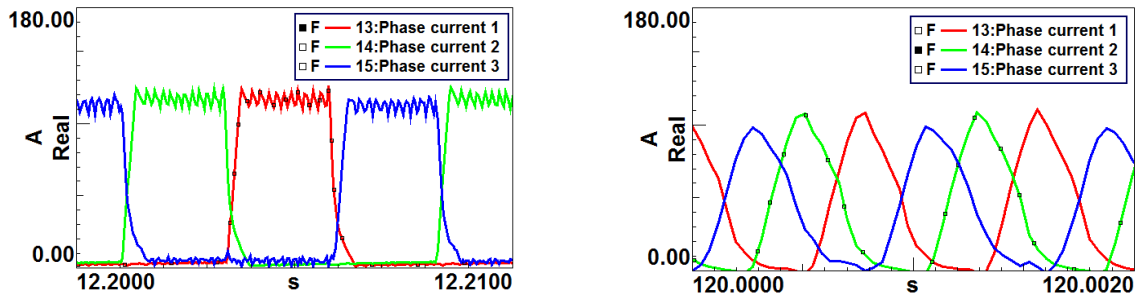

(a) Current wave form at low speed (b) Current wave form at higher speed

Figure 9 – Three phase current profiles

By removing the ripple on the current signal in the lower speed range the inverted C-shape is

disappeared. Figure 10 shows a part of the time traces for the original current wave form (red) and the modified current wave form without the ripple (blue) at a negative torque condition of - 49%.

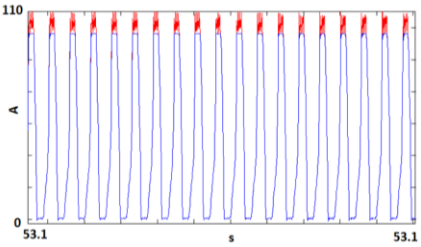

Figure 10 - Original current wave with ripple (red) and modified current wave without ripple (blue)

The corresponding waterfall plots are visualized in Figure 11. It can be noted that the inverted C-shape, has disappeared when the ripple is removed. Consequently, editing the current ripple gives a different content in terms of noise and vibrations.

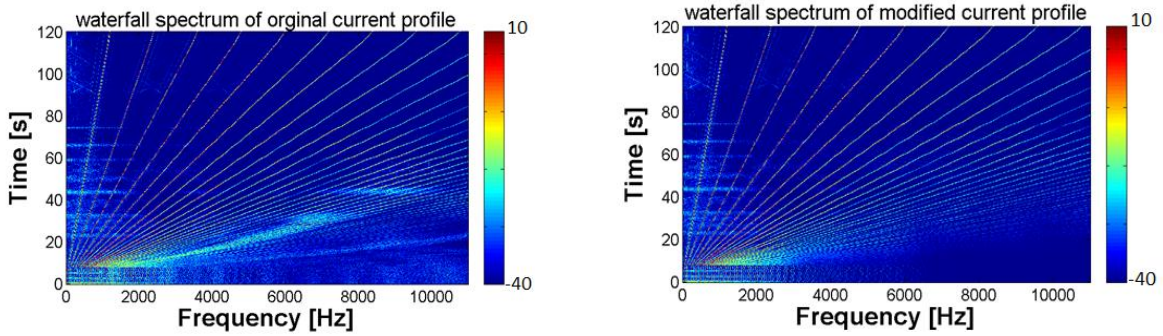

Figure 11 – Evaluation of the source of the inverted C-shape

The sound pressure level reaches its maximum when order 24 excites the ‘ovalization’ mode at 1330Hz. Hence, the claim that the ‘ovalization’ mode is not excited in a 12/8 SR motor and therefore doesn’t contribute to the acoustic noise, is not fully consistent with the practice: excitation of the ‘ovalization’ mode is still a major source of acoustic noise (Figure 12).

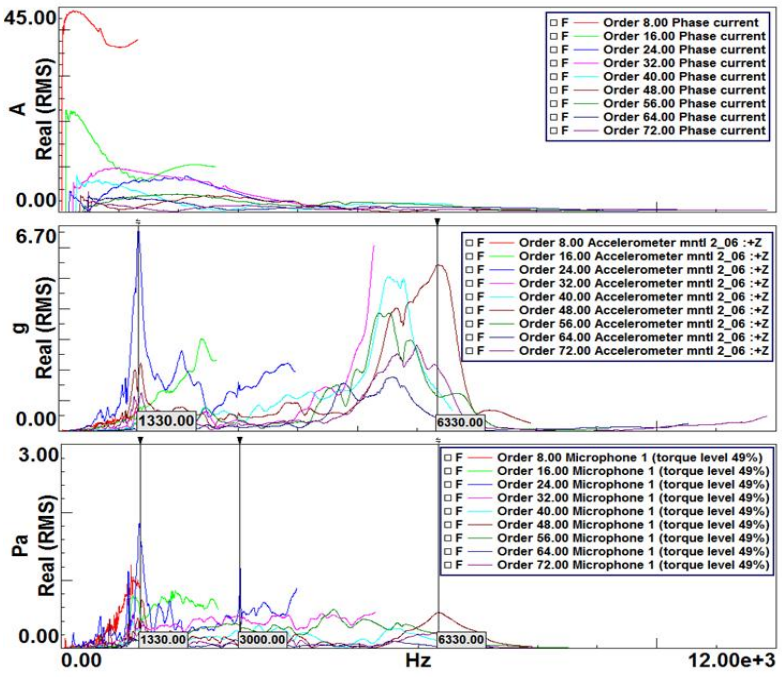

Figure 12 - Order sections of a phase current (top), an accelerometer (middle) and a microphone (bottom)

To verify the 'ovalization' mode shape, a modal analysis is carried out on the 12/8 SR motor. Results can be found in Figure 13a. All measurement conditions should be taken into account. Firstly, the modal analysis is performed on a complete SR motor including, stator, rotor, end shields, cooling water, etc. Secondly, the SR motor was clamped at one side. Consequently, this means that the measured mode frequencies (Figure 13) are a little bit different from the calculated FEM structural mode shapes (Figure 2b) because only the stator housing in free-free conditions is there considered.

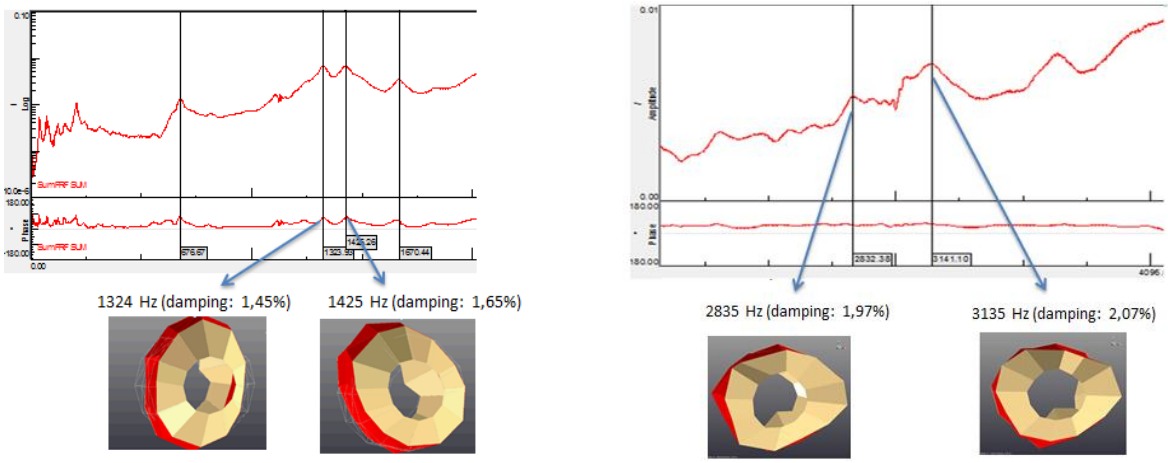

(a) Ovalization modes (b) Triangular modes

Figure 13 – Mode shapes obtained by modal analysis

Two 'ovalization' modes are presented (Figure 13a) at 1324Hz and 1425Hz. The 'ovalization' mode with out-of-phase of front/back is not presented due to the end shields. Measured resonance frequencies are higher and are more apart than simulated ones due to the end shields and clamping. The triangular modes (Figure 13b) at 2835Hz and 3135Hz are less visible because of the different boundary conditions between the measured and simulated modes. It was not possible to measure the square mode as the sampling frequency was too low during the modal analysis.

Finally, one resonance at 1330Hz in the frequency content of spectrograms in Figure 8 is confirmed by a modal analysis on the stator housing which visualizes the 'ovalization' mode at this frequency.

4.2 Deflection shapes and time domain animation

During the development process of a new electric motor, several numerical techniques, such as BEM and FEM, can be applied to characterize the dynamic properties. As shown in the discussion of the experiments, the mode shapes play an important role in the vibro-acoustic behavior of the motor. However, not all modes have equal importance. Furthermore, very often in operational conditions, the deformation of the structure doesn't correspond to a pure mode shape. Operational Deflection Shapes (ODS) can be used to evaluate the contribution of a mode during normal operating conditions. In this paragraph, the mode shapes are analyzed in terms of the dominant orders. For lowly damped structures, it can be proven that the form of the ODS highly corresponds to the real (modal) mode. For highly damped structures, the response of a certain frequency will also be contributed by other resonance frequencies. In other words, the resulting ODS will contain in this case different modes. The virtual reproduction of the mode shapes, carried out by an ODS analysis, is depicted in Figure 14 and Figure 15.

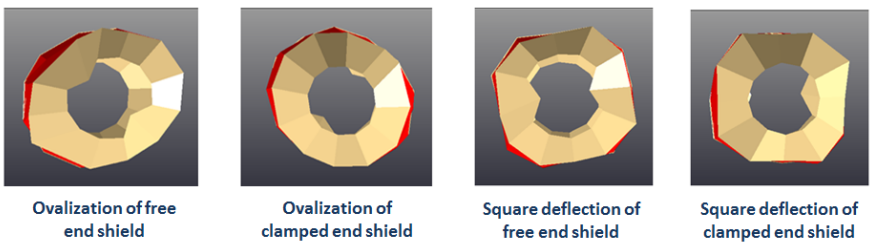

Figure 14 - Ovalization (above) at 3370 RPM and square (below) deflection shapes at 5120 RPM

The ‘ovalization’ deflection shape of the housing is visible in all orders at a particular frequency, RPM or time, but best in the 24th order. The ‘ovalization’ happens at both side panels. Both flanks move in phase with each other. The main difference with the modal analysis is that the effects of the mechanical structure behavior and excitation forces are now included during operational conditions. The square deflection shape is also visible in all orders, but the best in 56th order. Deflections happen at both side panels but they are less pronounced at the clamped flank, especially at higher speeds (Figure 15).

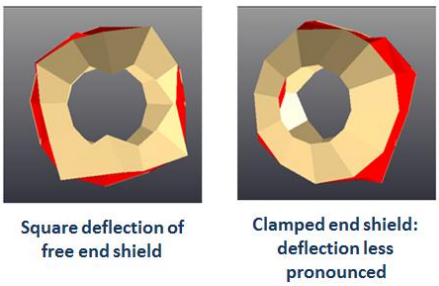

Figure 15 - Square deflection shapes at 5960rpm

4.3 Sound Quality evaluation

Characteristic for electric and hybrid vehicles is that their NVH performance is judged predominantly in noise perception terms rather than in noise levels. This is to a large extent due to the specific noise behavior of the electric drive systems, causing a higher annoyance than expected from the sound pressure level (5). The magnetic forces of the SR motor generate a typical tonal and high frequency noise, which is referred as whining noise. This source is the most dominant noise generated by the SR motor. Also other components of the SR motor are producing noise, as the unbalance of the rotor and the power electronics. The tonal and high frequency noise are annoying. This subjective appreciation can be more objectified by Sound Quality metrics. The ones used in this paper are: sharpness, tonality, loudness and prominence ratio. These values should be reduced for more pleasant sound in the vehicle. In Figure 16, three torque levels 0% (green), 6% (red), 49% (blue) are considered for a run between 0 and 9900 RPM.

A first valuable metric is tonality. The object of this metric is to evaluate the presence of tonal components in the spectrum of a noisy electric motor like a SR motor. Narrowband noises can also sound like tonal. The smaller the bandwidth is, the more tonal the noise propagates. Figure 16a shows a reproduction of the tonality. It can be noticed that the higher the torque level of the SR motor is, the higher the tonality of the sound is. Another feature which is relevant to the agreeableness of the sound of rotational devices is its sharpness. In this way, it is possible to classify sound as shrill (sharp) or ‘flat’. The sharpness can be expressed in the unit acum. When switching the SR motor on, a doubling of the sharpness is obtained, as shown in Figure 16b. The amount of noise coming from one microphone in different load conditions can also be expressed in sones instead of the more familiar decibel (Figure 16c). An advantage is that the sone scale is linear, meaning that doubling the amplitude corresponds to a doubling of the perceived loudness. As a result, it is easier to interpret the sound levels for the different torque levels.

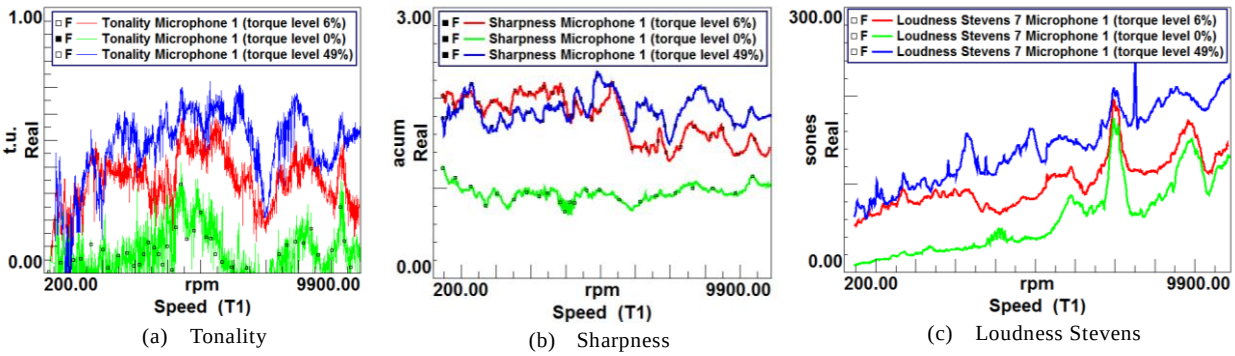

(a) Tonality (b) Sharpness (c) Loudness Stevens

Figure 16 – Sound metrics: tonality, sharpness, loudness Stevens VII

Figure 17 shows one example of the 'ovalization' mode confirmation in the acoustic noise based on a prominence ratio sound metric in different load conditions. In the prominence ratio method, a discrete tone nominee is said prominent if the average SPL of the 'critical band' centered on the tone is at least 9dB higher than the average SPL of the contiguous critical bands.

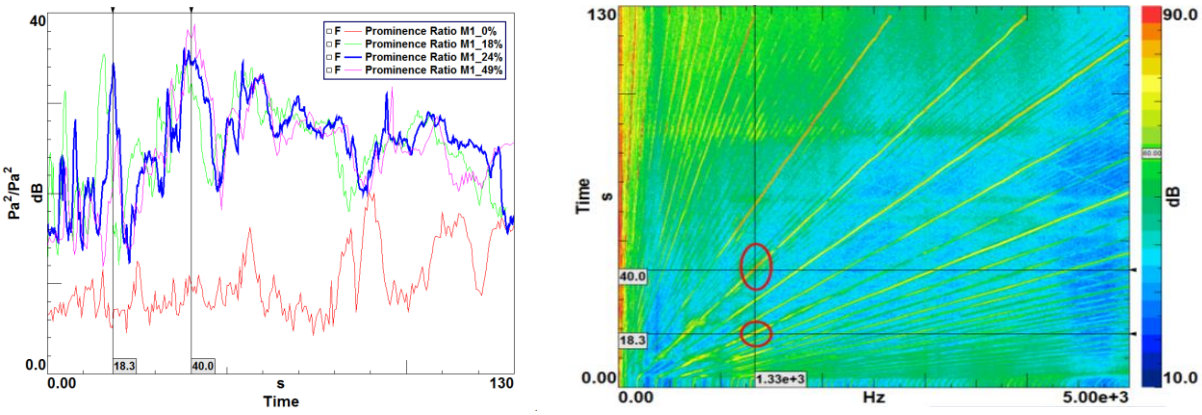

a) Sound metric: prominence ratio

b) Frequency content of one microphone near to the SR motor

Figure 17 – Sound metrics versus frequency spectra

Based on all these objectives techniques, it can be noticed that the torque level has a big effect on the tonality, the loudness and a smaller effect on the sharpness of the sound. In addition, prominence ratio can serve as a detection tool of the various stator mode shapes which are translated in the sound radiation. In this way, noise problems can be detected faster at a particular time, rotational speed and a known frequency which eventually enhances the optimization process of one typical problem.

5. CONCLUSIONS

Advanced NVH analytical tools, to analyze the spectral content of noise, current and vibrations in a 12/8 SR motor, have been introduced and applied to test rig measurements. In this way natural modes, harmonic components related to the motor construction and relations between measured signals are identified for a 12/8 SR motor. All these tools should help engineers in the future to gain insight in the vibro-acoustic behavior of electrical powertrains to optimize the NVH characteristics for automotive applications.

ACKNOWLEDGEMENTS

The presented research was achieved in the context of the research project Asterics –Ageing ad efficiency Simulation & Testing under Real world conditions for Innovative electric vehicle Components and Systems.

REFERENCES

1. Krishnan R., Switched Reluctance Motor Drives: Modeling, Simulation. CRC Press, 2001.
2. Dos Santos F.L.M., Anthonis J., Naclerio F., Gyselinck J., Van der Auweraer H., Sandoval Goes L., Multiphysics NVH Modeling: Integrated Simulation of a Switched Reluctance Motor Drivetrain for an Electric Vehicle, IEEE Transactions on Industrial Electronics, 61(1), 469 – 476, 2014, DOI 10.1109/TIE.2013.2247012.
3. Sarrazin M., Janssens K., Van der Auweraer H., Virtual Car Sound synthesis technique for brand sound design of hybrid and electric vehicles, SAE international 2012, 2012-36-0614 (2012)
4. Fiedler J.O. et. Al., Calculation of the Acoustic Noise Spectrum of SRM Using Modal Superposition, IEEE Transactions on Industrial Electronics, 57(2010), 2939-2945.
5. Van der Auweraer H., Meek B., Sarrazin M., Janssens K., NVH challenges with hybrid and electric vehicles, SAE International 2013-26-0511, Proc. SIAT, Pune, India, 9-12 Jan. 2013